A New Approach to Analyse Neighbourhood Relations in 2D Polygonal Networks

Lourenço Bandeira, Pedro Pina, and José Saraiva

CERENA-Centro de Recursos Naturais e Ambiente, Instituto Superior Técnico
Av. Rovisco Pais, 1049-001 Lisboa, Portugal

Abstract. A new algorithm to identify the neighbours of polygons on 4-connected raster images of 2D polygonal networks is presented in this paper. It is mainly based on mathematical morphology operators and can be indistinctively applied to networks of tri and tetravalent nature (with three and four edges at each vertex, respectively). The algorithm is tested on a varied set of polygonal terrains occurring on the surface of Mars and its computational performance compared to other approaches.

Keywords: Fast algorithm, mathematical morphology, topology, Mars.

1 Introduction

Polygonal networks are common in many surface analysis problems, from different fields of work, such as materials science, biology, geology and others. In the context of our research into a number of aspects of the surface of the planet Mars, we have come across countless examples of the presence of polygonal terrains [8]. These are commonly viewed as being related to the existence of water-ice in the ground, and to the seasonal cycles of freezing and thawing that it goes through. To study the many visually different polygonal patterns that occur on Mars [6], and try to find relations between their characteristics and the processes involved in their genesis, one of the possible approaches is to extract features related to their topology and geometry. The problem of the topological characterization of polygons has been addressed before and some parameters have been proposed to synthesize topological relations that exist in a given network [1,2,4,5,10]. The main step to obtain those values is the quantification of the first order neighbourhood for all polygons of the network. The classic approach to extract those topological relations [3] is applicable to all kinds of networks but, since it processes each polygon individually, it is very slow. A method that combined graph theory and mathematical morphology [9] was able to reduce significantly the computing time but, on the other hand, was unable to analyse the irregularity along the real edges of the polygons, since it works only for vectorial images (in which each real edge is represented by a single straight line). A more recent method [7], that is applicable to raster images and that processes all polygons at once, was able to reduce significantly the computing time, maintaining all the details of the edges, but was limited in its scope since it can only be correctly applied to trivalent networks.

J. Ruiz-Shulcloper and W.G. Kropatsch (Eds.): CIARP 2008, LNCS 5197, pp. 397–404, 2008.

Our current interest in studying polygonal terrains on the surface of Mars, which present extensive trivalent and tetravalent networks of large dimensions (a single network can include tens of thousands of polygons), led us to develop an alternative procedure to overcome the drawbacks of the previous approaches. This article takes on this problem, proposing a new robust algorithm based on mathematical morphology, faster than the classical approach but equally effective on 4-connected raster images of tri and tetravalent polygonal networks.

2 Previous Raster Algorithms

The algorithm proposed by Lantuéjoul in 1978 [3] (ALG1), used only mathematical morphological operators and consists of the individual identification of each cell in the network and the analysis of the neighbouring. Though this is a very simple algorithm, the computational performance depends directly on the number of polygons of the network under analysis.

The other approach, presented by Pina et al. in 1996 [7] (ALG2) and mainly based on morphological operators, was developed to study a trivalent material (cork cells), and to overcome the computational drawback of the previous approach. The simultaneous analysis of the vertices and the edges and their influence zones on the neighbouring cells permitted to obtain impressive computational improvements. However, a limitation of the method was found on the study of the neighbourhood of tetravalent vertices, due to the impossibility of dealing with some digital neighbourhood configurations, since only vertices with three edges could be correctly analysed.

3 New Algorithm

The approach herein presented (ALG3) applies mainly mathematical morphology operators, as the previous methods. The input binary images were obtained by a previous automated segmentation approach [8] which considers an unitary thickness for the segmented network with connectivity equal to four (c-4 rectangular grid). The method consists of the following steps:

1. Labeling all connected components i in the binary image of the polygons X:

$$X = \bigcup_i (X_i). \tag{1}$$

2. Identification of all the vertices $Ver(Y)$ in the complementary image of the polygons $Y = X^C$: this consists of applying a Hit-or-Miss Transform (HMT) with two neighbourhood configurations B that correspond to multiple points (Fig. 1), where 1 is a point belonging to an object or foreground, 0 is a point belonging to the background and $\bullet$ is a *don't care* point which means that it can belong to the foreground or to the background of the image:

$$Ver(Y) = HMT_B(Y) = \left\{ x | (B_{FG})_x \subseteq Y, B_{BG})_x \subseteq Y^C \right\}. \tag{2}$$

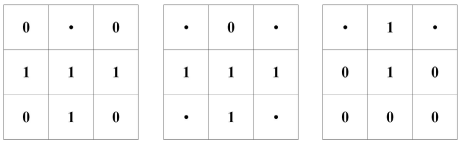

Fig. 1. Neighbourhood configurations corresponding to multiple points (left and centre) and extremities (right) on a 4-connected rectangular grid

where B_{FG_x} and B_{BG_x} correspond to the disjoint parts of the structuring element, respectively, in the foreground (FG) and background of the image (BG). An example of the detection of the vertices in a network is in Fig. 2b;

3. Resizing of images X and $Ver(Y)$, increasing its size by a factor of three, using a nearest-neighbour interpolation. This means that the line between adjacent polygons, now three pixels thick, has a boundary closer to each polygon and still maintains a one-pixel thick separation line between them;
4. Dilation δ of size 1 of all polygons X, to detect the external boundary of each polygon:
$$X_1 = \delta^{(1)}(X). \tag{3}$$
5. Intersection of the previous result X_1 with the vertices $Ver(Y)$, in order to mark the polygons in the neighbourhood of each vertex:
$$X_2 = X_1 \cap Ver(Y). \tag{4}$$
This operation permits to identify the polygons in the neighbourhood of each vertex or multiple point, as shown in Fig. 2c;
6. Removing of the extremities of the resulting elements; this operation is performed by a pruning of size 1, which is a thinning ($\bigcirc$), with the neighbourhood configuration E presented in Fig. 1(right):
$$PRUNE^{(1)}(X_2) = (X_2 \bigcirc E)^{(1)}. \tag{5}$$
The output of this step is shown in Fig. 2d;
7. Counting of the resulting pixels of the previous image in the labeled cells;
8. Repetition of steps 2, 4, 5, 6, and 7 for the particular situation where the neighbourhood configuration corresponding to a cross is found. This situation must be treated separately, since the corresponding vertex must reflect the presence of a diagonally opposed polygon, and thus must be counted once more. In Fig. 2e the result of the intersection of this specific configuration with the neighbouring polygons is shown;
9. Adding the result from step 7 to the one given by step 8. Thus, we obtain the correct number of first order neighbours for a connectivity of four, for each and every cell in the network. The resulting image is reduced three times in order to reconvert it to the original dimension (Fig. 2f).

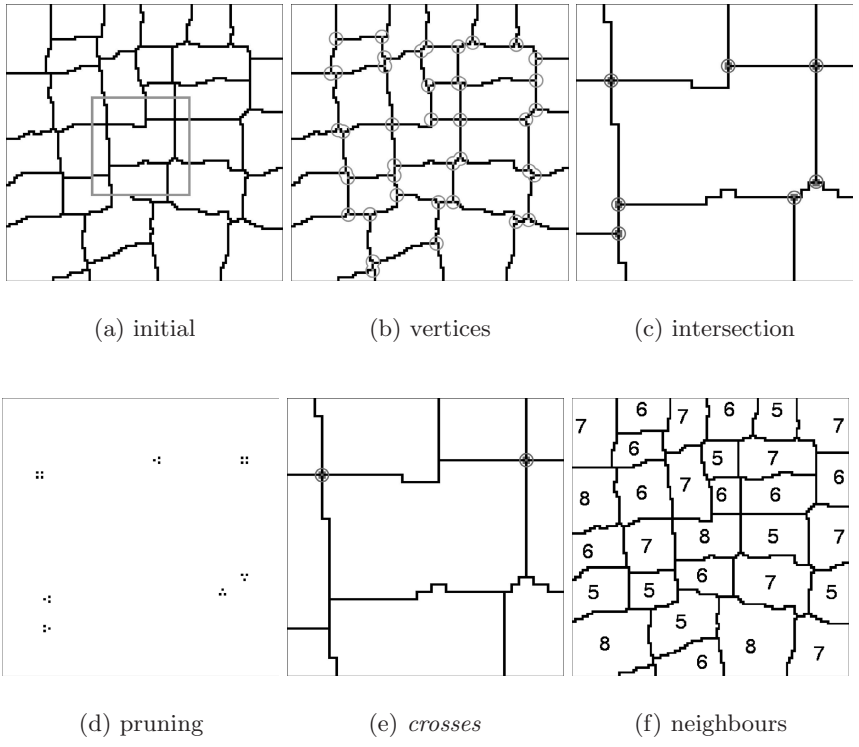

Fig. 2. Some steps of the algorithm ((c), (d) and (e) are performed and shown on resized network detail represented in (a); circles denote points of interest)

4 Results

The computational performance of the new algorithm (ALG3) is compared to that of the others mentioned above, first for a trivalent network example (ALG1 and ALG2), and then for the case of generic networks (only with ALG1). The computer used to obtain these processing times has the following characteristics: Intel®Core^{TM}2 Duo CPU, 2.66 GHz, 1.97GB of RAM.

4.1 Trivalent Networks

The trivalent network used consists of an 8-bit image of cork obtained with a Scanning Electron Microscope, with a dimension of 256 x 256 pixels (Fig. 3a), and whose cells are segmented with a dedicated approach [7] (Fig. 3b). The computation of the number of neighbours of every cell (Fig. 3c) gives the same results for all three algorithms but with different computing performances: ALG1 takes 0.802 seconds, ALG2 takes 0.203 seconds and ALG3 takes 0.375 seconds. The algorithm ALG1, that makes an individual cell analysis, is naturally the

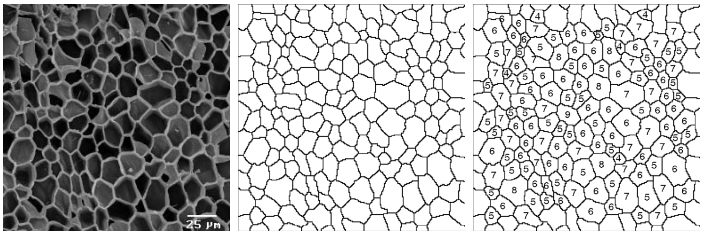

(a) input (b) segmented (c) neighbours

Fig. 3. Characterization of a trivalent network of cork cells

slowest, while ALG2 is the fastest (by a factor of 4). The new approach (ALG3) is slower than ALG2 but much faster than ALG1. The high similarity of cork cell networks in the images available, all with the same dimensions, does not allow us to go deeper in the analysis of those performances, namely as a function of the dimension of the images and the number of polygons therein contained. Therefore, this comparison will only be done for the martian terrains.

4.2 Generic Networks

Networks of trivalent and tetravalent nature are present in martian terrains. Given the countless different settings in which polygonal patterns occur on the surface of Mars, we decided to conduct a survey of narrow angle MOC (Mars Orbital Camera) images obtained by the NASA probe Mars Global Surveyor (MGS), acquired between 1998 and 2006, and to select interesting images according to the latitude of the centre of the image (higher than 50º, N or S) and its spatial resolution (better than 6 metres per pixel). The 15855 images that respected both of these criteria were all visually inspected to assess the presence of polygonal terrains which was verified for 1184 images; of these, those that presented adequate extensions of polygonal networks were chosen for analysis (188 images); 36 of these networks have been segmented and validated against ground-truth sets and constitute the dataset used in the following to evaluate our new algorithm. For illustrating purposes we present in Fig. 4 a set of six images of these martian patterns acquired by MOC/MGS.

The processing times, in seconds (s), for each of the corresponding segmented networks are presented in Table 1. The main general conclusion drawn from this table is that ALG3 is faster than ALG1, a fact that is confirmed for each of the 36 images studied so far, and that the time gap between them grows larger with the increase of both the number of polygons and the dimension of the image. For images with few polygons (like, for instance, image M19-01493 with 72 polygons) the performances of both algorithms are practically the same; but they become very different for images with higher numbers of polygons (like, for instance, the 6859 polygons in image M03-04266), where ALG3 is about one hundred times

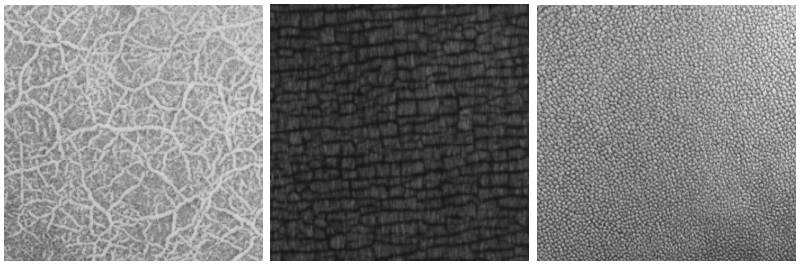

(a) E09-00029 (b) E10-01247 (c) M03-04266

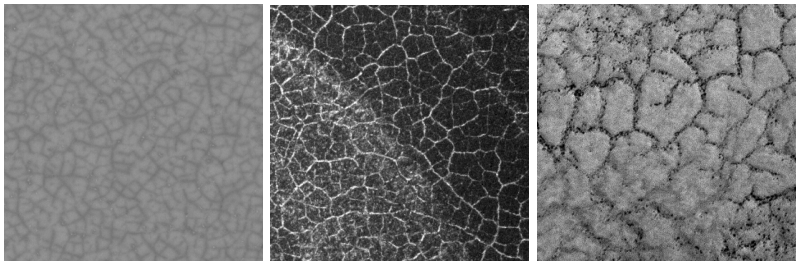

(d) M09-01292 (e) M09-06445 (f) M19-01493

Fig. 4. Samples of polygonal terrains on Mars (the side of each square image corresponds to 1 km on the terrain) [images NASA/JPL/MSSS]

Table 1. Performance on some martian images

Image Name	Size (pixels)	Polygons (number)	ALG1 (s)	ALG3 (s)	Times Faster
E09-00029	672 x 1948	1858	216.52	8.13	26.6
E10-01247	512 x 1636	10644	807.91	5.23	154.4
M03-04266	796 x 685	6859	248.92	2.45	101.5
M09-01292	512 x 3203	4364	647.30	10.13	63.9
M09-06445	648 x 1346	851	66.69	5.03	13.3
M19-01493	768 x 595	72	1.141	1.00	1.1

faster than ALG1, even though their dimensions are quite similar (768 x 595 pixels and 796 x 685 pixels, respectively).

A more generic evaluation of the performance of these two algorithms for all 36 networks available indicates that there is a direct correspondence between the processing time and the dimension of the images for ALG3 (Fig. 5a): the processing time increases linearly with the dimension of the images. If the product of the dimension of the images by the number of polygons present is plotted against the processing time, a similar linear behaviour is detected for ALG1 (Fig. 5b).

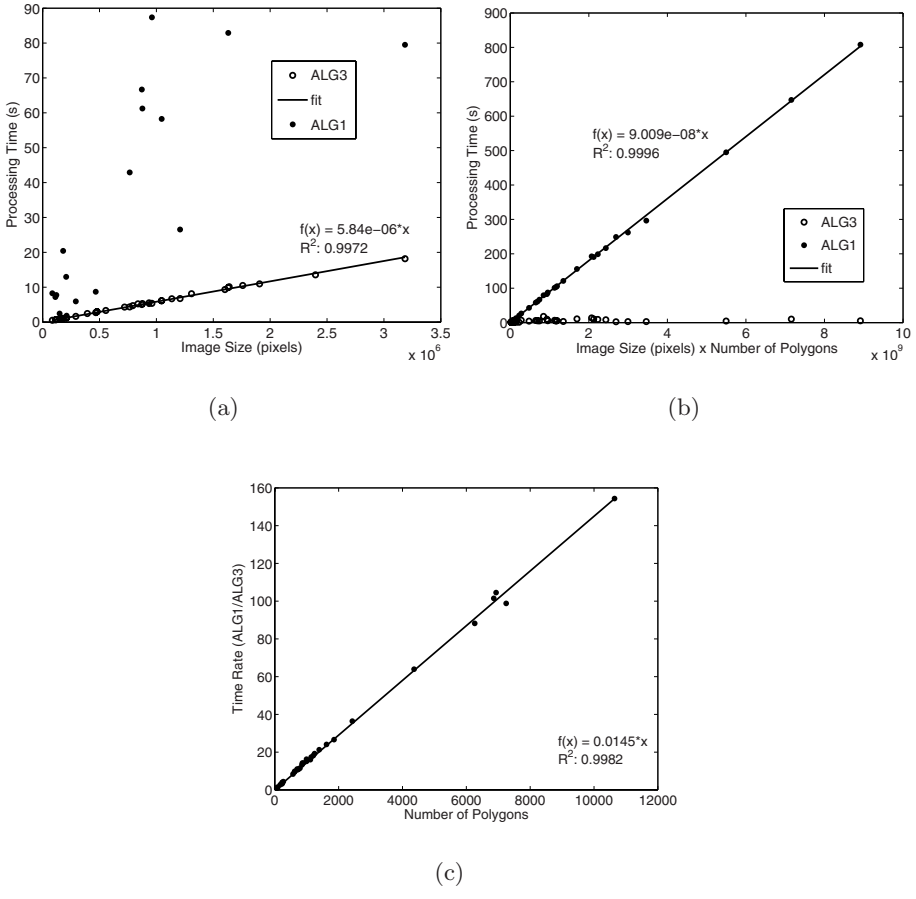

Fig. 5. Performances: (a) Processing Time vs. Image Size; (b) Processing Time vs. Image Size x Number of Polygons; (c) Time Ratio vs. Number of Polygons

Moreover, the time rate given by the ratio between the times of ALG1 and ALG3 also increases linearly with the number of polygons within each newtwork (Fig. 5c).

5 Conclusions

The main conclusions are that the proposed algorithm is of generalized application (for tri and tetravalent polygonal networks in 4-connected raster images) and the performances that it achieves are excellent. The varied set of MGS/MOC images herein used, with a spatial resolution between 1.5 and 6 metres, clearly demonstrates the usefulness of a faster approach to extract topological information of polygonal terrains. Furthermore, the benefits of this approach become clearer as the number of polygons in an image is larger.

The future use of images with a higher spatial resolution, like those that are currently provided by the HiRISE camera onboard the NASA probe Mars Reconnassaince Orbiter (MRO), where 25-30 cm/pixel are possible, will certainly benefit even more from this algorithmic improvement. In addition, the improved characteristics of the MRO camera show that polygonal terrains exist at smaller scales, not before observed on the surface of Mars, and more frequently than was previously thought. Thus, all improvements in speeding up the characterization algorithms, as well as the segmentation ones, must be seen as relevant and welcomed contributions.

Acknowledgments. This work was developed within the project TERPOLI (PTDC/CTE-SPA/65092/2006) funded by FCT, Portugal, which also supported LB (SFRH/BD/40395/2007) and JS (SFRH/BD/37735/2007).

References

1. Aboav, D.A.: The arrangement of grains in a polycrystal. Metallography 3(4), 383–390 (1970)
2. Aboav, D.A.: Arrangement of cells in a net. Metallography 13(1), 43–58 (1980)
3. Lantuéjoul, C.: La squelettisation et son application aux mesures topologiques des mosaïques polycristallines. Thése de doctorat. ENSMP, Paris (1978)
4. Lewis, F.T.: The correlation between cell division and the shapes and sizes of prismatic cells in the epidermis of Cucumis. Anatomical Record 38(3), 341–376 (1928)
5. Lewis, F.T.: A comparison between the mosaic of polygons in a film of artificial emulsion and the pattern of simple epithelium in surface view (cucumber epidermis and human amnion). Anatomical Record 50(3), 235–265 (1931)
6. Mangold, N.: High latitude patterned grounds on Mars: Classification, distribution and climatic control. Icarus 174(2), 336–359 (2005)
7. Pina, P., Fortes, M.A., Selmaoui, N.: Geometrical and topological characterization of cork cells by digital image analysis. In: Maragos, P., Schafer, R.W., Butt, M.A. (eds.) Mathematical Morphology and its Applications to Image and Signal Processing, pp. 458–466. Kluwer Academic Publishers, Boston (1996)
8. Pina, P., Saraiva, J., Bandeira, L., Barata, T.: Identification of martian polygonal patterns using the dynamics of watershed contours. In: Campilho, A., Kamel, M. (eds.) ICIAR 2006. LNCS, vol. 4142, pp. 691–699. Springer, Heidelberg (2006)
9. Vincent, L.: Graphs and mathematical morphology. Signal Processing 16(4), 365–388 (1989)
10. Weaire, D.: Some remarks on the arrangement of grains in a polycrystal. Metallography 7(2), 157–160 (1974)